Journal of the Serbian Chemical Society
JSCS-info@shd.org.rs • www.shd.org.rs/JSCS

ACCEPTED MANUSCRIPT

This is an early electronic version of an as-received manuscript that has been accepted for publication in the Journal of the Serbian Chemical Society but has not yet been subjected to the editing process and publishing procedure applied by the JSCS Editorial Office.

Please cite this article as K.T.S.N. Tarun Kumar, P. Peddi, M. V. Lakshmi, Ch. Rajyalakshmi, V. R. Anna, *J. Serb. Chem. Soc.* (2026) https://doi.org/10.2298/JSC260108063T

This "raw" version of the manuscript is being provided to the authors and readers for their technical service. It must be stressed that the manuscript still has to be subjected to copyediting, typesetting, English grammar and syntax corrections, professional editing and authors' review of the galley proof before it is published in its final form. Please note that during these publishing processes, many errors may emerge which could affect the final content of the manuscript and all legal disclaimers applied according to the policies of the Journal.

Journal of the Serbian Chemical Society
JSCS-info@shd.org.rs • www.shd.org.rs/JSCS
J. Serb. Chem. Soc. **00(0)** 1-17 (2026)
JSCS–13717
Original scientific paper
Published DD MM, 2026

Accepted Manuscript

Engineered cobalt-doped magnetic MOF@Ag_2O nanocomposites for adsorptive removal of polycyclic musk pollutants

K.T.S.N. TARUN KUMAR[1], PAVANI PEDDI[2], M.V. LAKSHMI[3], CH. RAJYALAKSHMI[4], AND VENKATESWARA RAO ANNA[1]*

[1]*Department of Chemistry, Koneru Lakshmaiah Education Foundation,Vaddeswaram, Guntur - 522302, A.P., India,* [2]*Department of Chemistry, FED, PVP Siddhartha Institute of Technology, Kanuru, Vijayawada-520007, A.P, India,* [3]*Department of Engineering Chemistry, S.R.K.R. Engineering College, Bhimavaram- 534204, A.P, India, and* [4]*Department of Basic Sciences, Vishnu Institute of Technology, Bhimavaram- 534202, A.P, India.*

(Received 8 January; revised 23 February; accepted 19 October 2026)

Abstract: Due to the increasing consumption of fossil fuels, there is a growing demand for renewable energy resources. At the same time, a significant amount of agricultural waste accumulates, including corn residues, and efficient management of this waste is a challenge. In this work, the waste biomass, which consisted of the stalks of two types of corn, was characterized and subjected to the pyrolysis process at 400 °C. Physicochemical characterization of the obtained liquid fraction (bio-oil) was performed, and the obtained data were compared with literature data for liquid biofuel. The calorific value of bio-oil was above 22 MJ kg^{-1}, which indicates the good potential of waste corn biomass as an energy source. With appropriate further changes in the composition of waste, by adding materials with a higher carbon and hydrogen content, corn stalks can represent a significant energy source, with better regulation of disposal and storage of agricultural waste.

Keywords: nanoscale; tonalide; galaxolide; adsorption kinetics; reusability.

INTRODUCTION

Contamination water by emerging organic pollutants was becoming significant environmental concern worldwide especially due to the widespread usage and persistence of synthetic chemicals in personal care and cosmetic products.[1] Among various synthetic chemicals, polycyclic musk fragrance compounds are widely used as fragrance additives in perfumes, shampoos, detergents, and other household items. These compounds are not only having chemical stability and lipophilic but also exhibit resistance to natural degradation processes and allows them to persist in aquatic environments long after their initial

* Corresponding author. E-mail: avrchemistry@gmail.com
https://doi.org/10.2298/JSC260108063T

use. The continuous release of these pollutants into environment through domestic wastewater effluents and industrial waste water can poses serious ecological and health threats such as endocrine-disrupting effects, bioaccumulation in aquatic organisms, and potential toxicity in higher trophic levels.[2]

These are micro-contaminants present at low concentrations, have complex structures, and exhibit strong chemical stability and hence the conventional wastewater treatment plants are not equipped to eliminate these contaminants effectively.[3]

Hence, polycyclic musks are frequently detecting at high levels in surface waters, sediments, and even drinking water sources. These issues encourage researchers to seek innovative and efficient materials for targeted removal of such pollutants and among the various innovations, adsorptive removal of considered as very effective due to its simplicity, cost-effectiveness, and non-destructive nature. However, the success of adsorption significantly depends on the development of high-performance adsorbent materials with specific surface properties, large surface area with reusable capability.[4] In recent years, metal-organic frameworks (MOFs) were garnered substantial interest in the field of environmental remediation.[5] The MOFs are crystalline porous materials that contain metal ions or clusters coordinated with organic ligands to form extended network structures.[6]

Their tunable pore sizes, high surface areas, and customizable functionalities make them ideal candidates to adsorb broad spectrum of environmental contaminants. However, MOFs exhibit low water stability and minimum adsorption efficiency toward certain hydrophobic pollutants. Hence there is a need to further functionalization or incorporation with other active components to enhance the adsorption efficiency.[7] These limitations were successfully addresses by incorporating magnetic nanoparticles (NPs) such as Fe_3O_4 or cobalt ferrite ($CoFe2O_4$) into the MOF matrix. Doping of Cobalt on to the MOF network enhance structural integrity and adsorption capacity through electronic interaction with adsorbate molecules and create more active sites. In parallel, silver oxide (Ag_2O) NPs shows significant potential for environmental remediation applications due to their high redox activity, photocatalytic properties, and antimicrobial capability.[8] The integration of Ag_2O into a cobalt-doped magnetic MOF structure presents a novel nanocomposite system with synergistic properties that can significantly enhance the removal of persistent pollutants like PCMs.[9] The microwave-assisted synthesis becomes an efficient approach in the fabrication of nanocomposites because this approach enables rapid and uniform heating, shortens synthesis time, improves particle dispersion, and facilitates strong interfacial interaction between composite components. These advantages make it particularly suitable to produce multifunctional MOF-based nanomaterials with enhanced structural uniformity and adsorption performance.

Accepted manuscript

Hence, the present work aims to bridge gap between advanced materials science and environmental remediation by developing a highly efficient and magnetically separable nanocomposite for removal of stubborn polycyclic musk fragrance pollutants such as galaxolide and tonalide. This work not only adds to the growing field of MOF-based environmental applications but also becomes best platform for future research into multifunctional nanomaterials with broader contaminant remediation capability.

MATERIALS AND METHODS

Materials and reagents

Silver nitrate ($AgNO_3$, CAS No. 7761-88-8, ≥99.9% purity), cobalt(II) nitrate hexahydrate ($Co(NO_3)2·6H2O$, CAS No. 10026-22-9, ≥98% purity), 2,6-pyridinedicarboxylic acid (CAS No. 499-83-2, ≥99% purity), N,N-dimethylformamide (DMF, CAS No. 68-12-2, HPLC grade, ≥99.8%), ethanol (CAS No. 64-17-5, analytical reagent grade, ≥99.9%), sodium hydroxide (NaOH, CAS No. 1310-73-2, pellets, ≥98%), calcium chloride ($CaCl_2$, CAS No. 10043-52-4, ≥96%), and sodium azide (NaN_3, CAS No. 26628-22-8, ≥99.5%) were purchased from Merck, Mumbai, India, and used as received without further purification. Deionized water was used throughout the synthesis and adsorption experiments. Galaxolide (CAS No. 1222-05-5, analytical standard, ≥98%) and Tonalide (CAS No. 1506-02-1, analytical standard, ≥98%) were obtained from Sigma-Aldrich and used as target polycyclic musk pollutants.

Preparation of extract

The earlier studies reported[10] was adapted for preparation of leaf extract of *Ficus carica* L., with minor changes. Fresh *F carica* L., leaves were collected, thoroughly washed with distilled water, and then rinse with ultra-pure water. The leaves were air-dried at room temperature for seven days and the dried leaves were ground into a fine powder using a grinder. Then 2 grams of leaf powder were mixed with 100 mL of deionized water and boiled at 70 °C for one hour. The mixture was then allowed to cool to room temperature and left to stand for 24 hours. Then, the extract was filtered through Whatman filter paper and stored in a refrigerator for future use.

Fresh leaves of *Ficus carica* L. were thoroughly washed with distilled water followed by ultrapure water to eliminate surface contaminants. The cleaned leaves were air-dried at ambient temperature for seven days and subsequently ground into a fine powder. Approximately 2.0 g of the powdered material was dispersed in 100 mL of deionized water and heated at 70 °C for 1 h under continuous stirring to facilitate the extraction of bioactive phytochemicals. After cooling to room temperature, the suspension was allowed to stand for 24 h to ensure complete extraction. Resulting extract was filtered through Whatman No. 1 filter paper and stored at 4 °C until further use.

Synthesis strategy.

The synthesis strategy adopted in this work comprises of three sequential steps. Initially, Ag_2O NPs were prepared through a green chemical precipitation approach using *Ficus carica leaf* extract as the reducing and stabilizing agent. Subsequently, Co-MOF was synthesized through solvothermal coordination reaction between cobalt nitrate and 2,6-pyridinedicarboxylic acid. Finally, Co-MOF@Ag_2O nanocomposite was fabricated through microwave-assisted deposition of Ag_2O NPs onto Co-MOF framework, followed by washing, drying, and calcination to obtain the final adsorbent.

Accepted manuscript

Green chemical precipitation synthesis of Ag_2O NPs.

The synthesis method was based on earlier studies reported with slight adjustments.[11] In this process, 10 mL of *F carica* L. leaf extract was mixed with 80 ml of 0.1 M silver nitrate solution (1.69 g) with continuous stirring. The pH level in the synthesis mixture was adjusted separately to 10 with addition of small amounts of NaOH. The precipitate formed in the reaction mixture was collected and dried in an oven at 90 °C. The dried material was further calcinated at 300 °C using a tubular furnace and the final product was stored for further analysis.

Solvothermal synthesis of Co-MOF

The precisely weighed 8.186 mmol of cobalt (II) nitrate was added to minimum amount of dimethylformamide (DMF) and 3.101 g of 2,6-pyridinedicarboxylic acid that serves as organic linker. The homogeneous reaction mixture was transferred into Teflon-lined stainless-steel autoclave and heated at 100 °C for 8 h under solvothermal conditions. It was naturally cooled to room temperature and resultant purple precipitate was collected by filtration, washed three times with DMF followed by ethanol, and dried at 100 °C for 12 h.[12]

Microwave-assisted synthesis of Co-MOF@Ag2O nanocomposite

In the preparation process of nanocomposite, 0.6 g of dried Co-MOF powder and 0.179 g (1 mmol) of Ag_2O was dispersed in deionized water. The mixture was stirred at 80 °C for 10 min to ensure uniformity. The resultant solution was transferred in to a glass vial and subjected to microwave irradiation at 300 W for 70 min. Then it was washed with acetic acid to remove any unreacted materials and the final product was dried in an air oven at 100 °C followed by calcination at 170 °C in a furnace.[12]

Co-MOF@Ag_2O nanocomposite was prepared through microwave-assisted integration of Ag_2O nanoparticles with the Co-MOF framework. Briefly, 0.6 g of the synthesized Co-MOF and 0.179 g (1 mmol) of Ag_2O nanoparticles were dispersed in deionized water and magnetically stirred at 80 °C for 10 min to obtain a homogeneous suspension. The mixture was transferred to a sealed glass vial and subjected to microwave irradiation at 300 W for 70 min to promote uniform deposition of Ag_2O onto the Co-MOF surface. Obtained nanocomposite was washed with dilute acetic acid to remove unreacted species, followed by repeated washing with deionized water. Finally, the material was dried at 100 °C and calcined at 170 °C to obtain the Co-MOF@Ag_2O nanocomposite.

Characterization of Co-MOF@Ag_2O nanocomposite

Fourier-transform infrared (FT-IR) spectra were recorded using potassium bromide (KBr) pellets within the range of 400 to 4000 cm^{-1} on a Bruker (USA) spectrophotometer. The X-ray powder diffraction (XRD) was carried out using a Bruker (USA) D8 diffractometer with Cu Kα radiation (2θ of 20-100°) and a graphite monochromator to examine the crystalline nature of the sample. Surface structure and morphology were studied using a scanning electron microscope (Jeol 6390LA, Japan) equipped with an energy-dispersive X-ray spectroscopy (EDX) unit. Thermal stability of nanocomposite was evaluated through a nitrogen atmosphere from room temperature up to 350 °C using a Mettler Toledo (India) thermal analyzer. Nitrogen adsorption–desorption measurements for surface area and porosity were performed using BET analyzer.

Adsorption studies

The Batch sorption experiments[13,14] was performed in triplicates to assess adsorption efficiency of synthesized Co-MOF@Ag_2O Nanocomposite for adsorption of polycyclic musk compounds such as Galaxolide and Tonalide. The 1 g/L concentration of both musk compounds

Accepted manuscript

was prepared separately in methanol and the methanol solvent interference was prevented by maintaining 0.1 % concentration in the experimental solution. In the reaction mixture, calcium chloride (0.005 mol/L) and sodium azide (100 mg/L) solutions were added to maintain consistent ionic strength and reduce microbial growth respectively. In each test, 50 mg of nanocomposite was added to 40 mL of a 2 mg/L of musk compound solution in amber glass vials. These vials were sealed and shaken at 100 rpm for 90 min at room temperature using a rotary mixer. After the reaction period, samples were filtered using 0.22 µm cellulose nylon membrane filters, and the remaining musk compound concentration in the filtrate was measured. The amount of musk compound adsorbed was determined by subtracting the final concentration from the initial one. Adsorption efficiency was compared by running a control experiment without addition of any adsorbent. [0-23]

The initial pH of the adsorption solution was adjusted to target pH using dilute HCl or NaOH before the addition of the adsorbent. The ionic strength throughout all adsorption experiments was maintained at a constant value using 0.005 mol/L $CaCl_2$ as the background electrolyte. No buffer system was employed because buffering agents may interact with the adsorbent surface or compete with the target analytes for active adsorption sites and thereby influences the adsorption process. Therefore, the initial pH was carefully adjusted and monitored throughout the experiments while maintaining constant ionic strength.

30 mg of nano-adsorbent was mixed with 40 mL of Musk compound solution at different concentrations in 0 to 5 mg/L range to assess the adsorption behavior of musk compounds using nanocomposite. The mixtures were left to reach equilibrium over 90 min and the quantity of compound adsorbed (R in %) was determined for both compounds using the formula 1 and the adsorption equilibrium (q_e) was determined using formula 2.

$$R\ (\%) = [(C_i - C_e) \times V / C_i] \times 100 \quad (1)$$

$$q_e = (C_i - C_e) \times V / m \quad (2)$$

In the equation, C_i and C_e represents the initial and equilibrium concentration of musk compound, V represents the musk compound solution taken for adsorption study in L and m will be the weight of nanocomposite utilized as adsorbent.

Two kinetic models such as Lagergren pseudo-first-order and the pseudo-second-order models were utilized to understand the adsorption process of musk compounds using the synthesized nanocomposite. The kinetic equations are as follow

$$Ln\ (q_e - q_t) = \ln (q_e) - K_1 \cdot t \quad (3)$$

$$t/q_t = 1 / (K2 \cdot qe^2) + t / q \quad (4)$$

In this equation, q_t (mg/g) is the adsorption amount at time t, q_e (mg/g) is the amount adsorbed at equilibrium. K_1 (min^{-1}) and K2 ($g \cdot mg^{-1} \cdot min^{-1}$) is the rate constant for the first-order and second order model respectively.

Analysis of musk compounds

Gas chromatography–mass spectrometry (GC-MS) system analysis was performed to assess the quantity of musk compound in the stock solution, after nanocomposite treated solution.[24] Results observed in this study were utilized to evaluate the adsorption efficiency of synthesized nanocomposite for the adsorption of musk compounds in the study. The experiment was conducted on GC (Agilent, 6890N) with mass selective detector (Agilent, 5975).[25] Analysis was performed in electron ionization mode at 80 eV with a scan range of 50 to 1000 amu and 2 scans/second scan rate. Separation was achieved on a DB-5 capillary column (30 m × 0.25 mm; 25 µm) using Helium as carrier gas at a flow rate of 1.0 mL/min. The injection port and detector

Accepted manuscript

temperatures were maintained 230 °C and 250 °C respectively. Oven temperature was initially set at 150 °C and this temperature was programmed to raise 15 °C/min up to a final temperature of 270 °C. The musk compound was injected at an injection volume of 1 µL using a splitless mode.

All adsorption experiments were performed in triplicate, and the results are expressed as mean ± standard deviation (SD). The statistical analysis was carried out using one-way analysis of variance (ANOVA), and differences were considered statistically significant at $p < 0.05$

RESULTS AND DISCUSSION

This study intended to synthesize Co-MOF@Ag_2O nanocomposite for the removal of polycyclic musk compounds such as Galaxolide and Tonalide. A noticeable color transformation was observed during the synthesis of Ag_2O NPs, Co-MOF and Co-MOF@Ag_2O nanocomposite indicate the successful formation of desired products. In the process of green synthesis of Ag_2O NPs, the initial pale color of the silver nitrate was change to dark brown color due to the addition of *Ficus carica* L., leaf extract. This indicates the reduction of Ag^+ ions and the formation of silver oxide NPs and the addition of NaOH raise the pH to 10 and further promote precipitation. A dark brown to black precipitate formed was collected after completion of reaction to achieve stable Ag_2O NPs. In the synthesis of Co-MOF, the initial solution was deep pink due to the presence of cobalt (II) ions in dimethylformamide. Upon the addition of 2,6-pyridinedicarboxylic acid and subsequent heating at 100 °C, the solution gradually turned into a purplish suspension, indicating complex formation between the cobalt ions and organic linker.[12] The integration of Ag_2O with the Co-MOF framework was confirmed by visualizing blackish in appearance in the reaction mixture. The morphological, structural and elemental characterization of synthesized nano-composite was assessed through various characterization techniques.

The initially colorless to pale silver nitrate solution gradually changed to dark brown upon the addition of *Ficus carica* leaf extract, indicating the formation of silver oxide nanoparticles. This color change is attributed to the reduction of Ag^+ ions by phytochemicals such as polyphenols, flavonoids, terpenoids, and reducing sugars present in the leaf extract. These biomolecules donate electrons to silver ions, resulting in the formation of Ag_2O nanoparticles while simultaneously acting as capping agents that stabilize the nanoparticle surface and prevent excessive aggregation. Under alkaline conditions (pH 10), Ag^+ ions initially react with hydroxide ions to form AgOH, which rapidly dehydrates to Ag_2O according to the reaction:

$$2Ag^+ + 2OH^- \rightarrow Ag_2O(s) + H_2O$$

The characteristic dark brown coloration is therefore considered visual evidence of nanoparticle formation and is consistent with previous reports on the green synthesis of silver oxide nanoparticles using plant-derived phytochemicals.[11]

Accepted manuscript

XRD results Fig. 1 confirms that the synthesized Ag_2O nanoparticles exhibit a polycrystalline structure with a cubic phase. The prominent diffraction peaks observed at the 38.7° (111), 43.9° (200), 64.5° (220), and 77.9° (311) and these planes are in good agreement with the standard face-centered cubic structure of Ag_2O (JCPDS Card No. 04-0783). XRD pattern of Co-MOF also displays several sharp peaks, indicate its polycrystalline nature. The crystallite size was calculated using Scherrer's equation i.e

$$D = K \lambda / \beta \cos \theta \quad (5)$$

In the equation D is the average crystallite size, in nm, K is the shape factor, λ represent the X-ray wavelength, β is the Full Width at Half Maximum of the diffraction peak and θ will be the Bragg diffraction angle (in degrees). Based on this calculation, the average crystallite size of the Co-MOF@Ag_2O nanocomposite was observed as 26.9 nm and results indicate good particle distribution and uniformity.

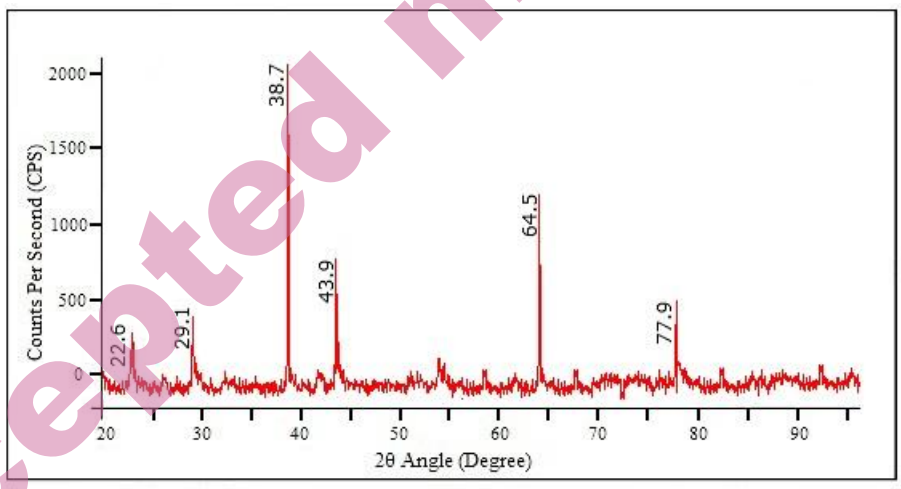

Fig. 1. XRD pattern of synthesized nanocomposite

EDX analysis was conducted to confirm the elemental composition of the synthesized nanocomposite Fig. 2. EDX spectrum shows a strong and distinct peak around 3 keV, which corresponds to the Ag Lα emission line. Additionally, a smaller Ag Lβ peak was also noticed in the spectrum confirms the successful incorporation of silver (Ag) into the composite. The noticeable Kα emission at approximately 6.9 keV was observed in the spectrum prove the presence of Co as organic ligand framework. Quantitative analysis confirms that cobalt is the most abundant element in the composite with a weight percentage of 61.52±0.001 %. The elements correspond to plant-derived reducing agents such as oxygen (O), nitrogen (N), and carbon (C) were noticed at lower amounts of 2.57±0.004 %,

Accepted manuscript

1.32±0.013 %, and 0.71±0.005 % respectively confirms the biological synthesis of nanomaterial. Presence of nitrogen and oxygen in the nanocomposite confirms the successful coordination of the organic linker with cobalt ions. EDX results observed in this study was in correlation with findings reported in literature.[14]

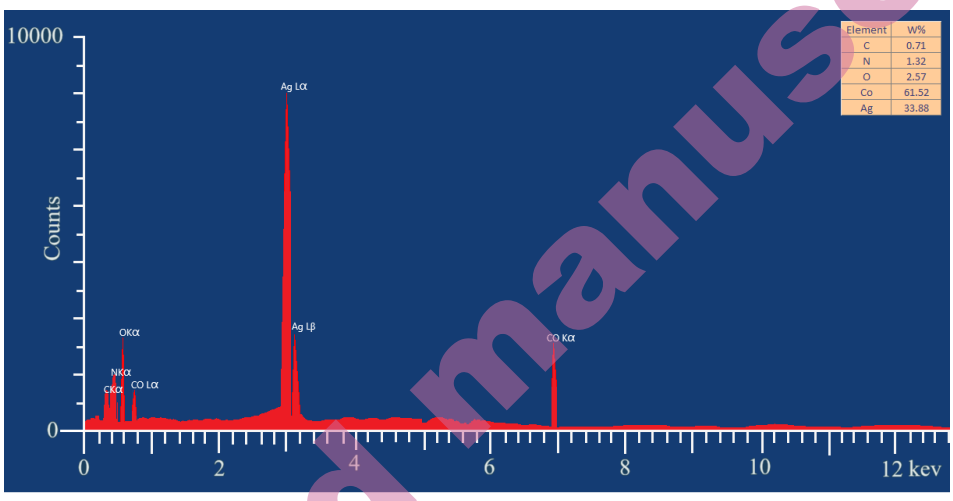

Fig. 2. EDX spectra of synthesized nanocomposite

Surface morphology of the synthesized Co-MOF@Ag_2O nanocomposite was examined using SEM and result was depicted in Fig. S1a. The SEM analysis reveals that the nanocomposite consists of nearly spherical particles with uniform distribution and a tendency to form aggregates. These particles appear well-structured with smooth surfaces, and the particle size in 26 to 32 nm proved the nanoscale dimension of the synthesized material. The aggregation observed in the SEM image may be due to interparticle interactions that are commonly observed in bimetallic or composite nanostructures. Zeta potential analysis was conducted to determine the surface charge and colloidal stability of the nanocomposite in water. The nanocomposite exhibits a zeta potential of –32 mV (Fig. S1b) that reflects a relatively high negative surface charge. This negative charge reflects good electrostatic stability and particle-to-particle repulsion in suspension that inhibits excessive agglomeration. The intense negative zeta potential also suggests the existence of surface functional groups from the phytochemicals of *Ficus carica* leaf extract that acquire surface charge. The SEM and zeta potential analyses collectively establish the formation of stable, nanosized Co-MOF@Ag_2O particles with good colloidal stability.

Thermal behavior of the synthesized Co-MOF@Ag_2O nanocomposite was investigated through thermogravimetric analysis. The TGA curve as shown in Fig. S2 reveal a gradual and continuous weight loss from room temperature up to

Accepted manuscript

approximately 500 °C, indicates a multistep decomposition process. Initial mass loss of approximate 3.5±0.002 % was observed around 100 °C due to the evaporation of physically adsorbed moisture and any residual solvents from the synthesis process. This low-temperature loss confirms the presence of volatile surface molecules due to the use of deionized water and plant extract in the synthesis of nanocomposite. A more significant weight loss of about 14.9±0.121 % and 21.1±0.003 % was observed between 250 °C to 300 °C due to the thermal decomposition of organic components used in the Co-MOF framework. This decomposition confirms the breakdown of organic bonds within the MOF structure and a subsequent mass reduction noticed after 300 °C may be due to the release or breakdown of coordinated water molecules and residual organic species tightly bound within the nanocomposite matrix. The relatively slow and stepwise thermal degradation confirms that the Co-MOF@Ag_2O nanocomposite has good thermal stability and this stability is advantageous for its potential use in high-temperature catalytic or adsorption applications. Thermal behavior noticed in thermogravimetric analysis was in aligns with the structural robustness observed in SEM and XRD analyses proves the composite's integrity and functional potential of nanocomposite.

Adsorption studies

Adsorption capacity of the synthesized Co-MOF@Ag_2O nanocomposite was tested with two polycyclic musk compounds namely Galaxolide and Tonalide. These two compounds are recognized as environmental pollutants based on their persistence and bioaccumulative potential. Adsorption experiments were conducted in triplicates to guarantee reproducibility and precision of data. Nanocomposite's removal efficiency against the target analytes was evaluated by determining the residual concentration of musk compounds at different time intervals through GC-MS.

Standard solutions of Galaxolide and Tonalide were initially prepared and characterized to determine their respective retention times and to prepare calibration curves. With the given GC conditions, Galaxolide and Tonalide were found to elute at retention times of about 11.1 and 7.0 minutes respectively. These were used as reference points for the identification of the compounds in the experimental samples. The calibration curves for Tonalide and Galaxolide were prepared using standard solutions within 0.2–1.2 µg/mL concentration range. Excellent linearity was achieved for both analytes, with coefficients of determination (R^2) of 0.9991 for Tonalide and 0.9994 for Galaxolide. The resulting calibration equations were subsequently used for the quantitative determination of the residual concentrations of both analytes during the adsorption experiments.

During the adsorption experiment, 5 mL aliquots of reaction mixture at every 5 minutes intervals were withdrawn, filtered to get rid of the adsorbent, and analyzed by GC-MS. The amount of compound adsorbed was determined from the

Accepted manuscript

decrease in relative peak area. [19] The diminishing trend of peak intensities of Galaxolide and Tonalide in the chromatograms with time validated the successful adsorption by the Co-MOF@Ag_2O nanocomposite. As indicated by Fig. S3, the chromatograms present a definite decrease in the peak areas of the musk compounds, reveals time-dependent adsorption behavior. These findings prove that Co-MOF@Ag_2O nanocomposite has a high affinity toward these contaminants and imply its huge potential as an excellent material for environmental cleanup of synthetic fragrance impurities.

The pH of solution produces significant influence on the adsorption efficiency of both the compounds in the study Fig. S4a. At low pH value of 2–3, the minimal adsorption percentage of 12.5±0.016 – 14.2±0.174 % was noticed for Tonalide and 9.6±0.236 – 11.8±0.361 % was for Galaxolide. This low adsorption may be due to excessive protonation of the adsorbent surface that leads to reduced interaction between the nanocomposite and the hydrophobic analytes. The reduction in adsorption efficiency under acidic conditions was may also be due to partial aggregation of the nanocomposite particles. At low pH, protonation of the surface can decrease electrostatic repulsion between particles. This repulsion promotes aggregation and reduces the effective surface area and availability of active adsorption sites. Furthermore, excess H^+ ions may compete with target analytes for adsorption sites and contribute to the lower adsorption efficiency observed at acidic pH. As the pH increases to 4–6, adsorption efficiency significantly improves and a maximum adsorption of 81.3±0.231 % was noticed for Tonalide at pH 5 whereas 84.6±0.418 % was noticed for Galaxolide at pH 6. One-way ANOVA indicated that the increase in adsorption efficiency with increasing pH was statistically significant ($p < 0.05$). The data are presented as mean ± SD ($n = 3$). This improvement is likely due to optimal surface charge condition that enhances the π–π interactions, van der Waals forces, and hydrophobic interactions. At these pH levels, the surface of Co-MOF@Ag_2O is less protonated that allows better accessibility and stronger binding of the musk compounds. Adsorption efficiency was noticed to be declined for both compounds at higher pH values of 7 – 9. The adsorption drops sharply from 64.6±0.027 % at pH 6 to 31.5±0.103 % at pH 7, and continues decrease to 13.1±0.213 % at pH 9 for Tonalide. A similar trend was observed for Galaxolide, with % adsorption reduces from 84.6±0.418 % at pH 6 to 28.9±0.213 % at pH 9. This decline may be attributed to the increase in negative surface charge of the adsorbent at alkaline pH that leads to electrostatic repulsion and reduced interaction with the neutral or weakly polar analytes. This result suggests that, pH 5 and 6 was concluded to be optimal pH for the adsorption of Tonalide and Galaxolide respectively.

The pH-dependent BET surface area or particle dispersion measurements were not performed in the present study. The partial aggregation of the nanocomposite under acidic conditions may reduce the effective surface area and

Accepted manuscript

the accessibility of adsorption sites and thereby contribute to the observed decrease in adsorption efficiency. This represents a limitation of the present study, and future investigations through pH-dependent BET surface area and particle dispersion analyses would provide further insight into the adsorption mechanism.

Optimal dose of the nanocomposite for the adsorption of Tonalide and Galaxolide was assessed through batch adsorption experiments. These experiments were conducted using an adsorbent dosage of 5–50 mg/100 mL, initial analyte concentration of 2 mg/L, optimized pH values of 5 for Tonalide and 6 for Galaxolide. In each adsorbent dosage, the adsorption mixtures were kept under identical conditions for 90 min to achieve equilibrium before evaluation of adsorption efficiency. These results indicate a significant increase in adsorption efficiency with increasing adsorbent dose up to 20 mg. The % adsorption of Tonalide increases from 43.4±0.107 % at 5 mg to a maximum of 89.7±0.043 % at 20 mg whereas Galaxolide adsorption increases from 39.7±0.107 % to 88.4±0.117 % over the same dose range Fig. S4. However, further increase in adsorbent dose of above 20 mg led to a slight decline or plateau in adsorption efficiency, with Tonalide shows 81.5±0.003 %, 78.6±0.106 %, and 79.1±0.244 % at 30, 40, and 50 mg, respectively whereas Galaxolide maintain nearly constant efficiency around 85±0.002 %. This decline at higher doses may be attributed to agglomeration of adsorbent particles can overlap the active sites that result in reduced effective surface area. Therefore, the optimal dose of nanocomposite for maximum removal of Tonalide and Galaxolide was proved to be 20 mg/100 mL and 30 mg/100 mL respectively.

The influence of contact time on adsorption efficiency of Tonalide and Galaxolide onto the nanocomposite was evaluated by performing batch adsorption experiments at a contact time of 5 to 180 min. The initial analyte concentration (2 mg/L), adsorbent dose, solution pH and solution pH were kept constant throughout the study. Results reveal that the adsorption of both compounds increased rapidly during initial phase of the contact period. In this period, the percentage adsorption of Tonalide was increased from 35.8±0.124 % (5 min) to 89.7±0.043 % (30 min) whereas the adsorption of Galaxolide was increased from 29.91±0.099 % to 78.92±0.137 % within 30 minutes Fig. 1. Rapid uptake in the first 30 min can be attributed to the availability of abundant active sites on the adsorbent surface. In this time, the large number of active sites on the surface of adsorbent facilitates the fast binding of hydrophobic Tonalide and Galaxolide molecules and the rate of adsorption slows down due on the increase of time due to saturation of active sites and reduced diffusion of molecules into deeper pores of the composite structure. Further, the porous architecture of MOF enhances the accessibility of target compounds, while the presence of Ag_2O may contribute to specific surface interaction that improves the adsorption affinity. Finally, the Tonalide adsorption of over 95 % and 97 % of Galaxolide adsorption was achieved by 90 minutes

Accepted manuscript

indicate that this duration is sufficient for near-complete removal of both compounds. Hence, the contact time of 90 minutes was considered as optimal for effective adsorption of selected pollutants.

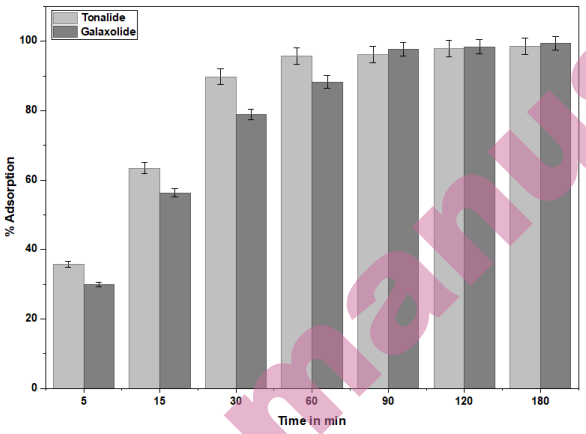

Data are presented as mean ± SD (n = 3). Error bars represent one SD ($p < 0.05$)

Fig.1. Results observed in adsorptive removal study of musk compounds using nanocomposite synthesized in this study

Pseudo-first-order and pseudo-second-order kinetic models were utilized to understand the adsorption mechanism and rate-controlling steps involved in the adsorption of studied pollutants using synthesized Co-MOF@Ag_2O nanocomposite. The kinetic data observed for Tonalide and Galaxolide were first fitted to the pseudo-first-order model and this model produce a correlation coefficient (R^2) of 0.926 and 0.979 for Tonalide and Galaxolide respectively Fig. S5a suggest a moderate fit. This indicates this model partially describes the adsorption behaviour and it does not fully represent the actual mechanism of adsorption. The pseudo-first-order rate constant (k_1) was calculated to be 0.0376 and 0.0379 min^{-1} for Tonalide and Galaxolide respectively. In contrast, the data shows an excellent fit to pseudo-second-order model with a high R^2 of 0.9989 and $R^2 = 0.999$ Fig. S5b with pseudo-second order rate constant (k_2) of 0.001165 and 0.000679 g/mg/min for Tonalide and Galaxolide respectively indicates a superior fit. The calculated equilibrium capacity (Q_e) was noticed to be 105.41±0.263 mg/g and 110.10±0.115 mg/g for Tonalide and Galaxolide respectively. This suggests that the adsorption of Tonalide onto Co-MOF@Ag_2O nanocomposite follows a pseudo-second-order kinetic behavior and is likely governed by chemical interactions that involve π–π stacking, hydrogen bonding, or coordination with active metal sites.

Adsorption equilibrium data of Galaxolide using synthesized Co-MOF@Ag_2O nanocomposite was assessed through Langmuir and Freundlich

Accepted manuscript

isotherm models. The isotherm results provide the adsorption mechanism and surface interaction characteristics of Galaxolide adsorption using Co-MOF@Ag_2O. Langmuir isotherm Fig. S6a displays the high F-value of 851.33 with highly significant Prob > F of < 0.0001 and very low residual sum of squares (1.72×10^{-5}). The model displays strong liner fit with R^2 of 0.9953 and an adjusted R^2 of 0.9942 confirms the applicability of monolayer adsorption on a homogeneous surface. The maximum monolayer adsorption capacity (q_m) was observed to be 229.55 mg/g with Langmuir constant (KL) of 0.1836 L/mg. Results indicate the high affinity between Galaxolide and the active adsorption sites of the Co-MOF@Ag_2O nanocomposite. Similarly, the Freundlich isotherm Fig. S6b also demonstrates an excellent fit with F-value of 975.80, a statistically significant Prob > F of < 0.0001 and a residual sum of squares of 0.05427. This model also exhibits R^2 of 0.9959 and an adjusted R^2 of 0.9949. These results confirm that the surface heterogeneity and multilayer adsorption may also contribute to the overall adsorption process. Collectively, these results confirm that both isotherm models adequately describe the adsorption behaviour with Langmuir as most performing model suggest that the monolayer chemisorption was the predominant mechanism for the adsorptive removal of Galaxolide using synthesised Co-MOF@Ag_2O nanocomposite.

Langmuir and Freundlich isotherm models were adopted to evaluate the adsorption mechanism of Tonalide using the synthesized Co-MOF@Ag_2O nanocomposite. Langmuir isotherm produces very low residual sum of squares of 1.72×10^{-5} with high R^2 value of 0.99532 and an adjusted R^2 of 0.99415 Fig. S6c. Linearized Langmuir plot produces an intercept value of 0.02214 and a slope of 0.005. These statistical values reflect the well-defined monolayer adsorption behavior of Tonalide on the uniform surface of nanocomposite. The F-value of 851.33 and a highly significant Prob > F value of < 0.0001 was observed further confirm the reliability of the Langmuir model. In comparison, the Freundlich isotherm also provides the good linear fit with an R^2 value of 0.9867 and an adjusted R^2 of 0.98337, along with residual sum of squares of 0.16147 Fig. S6d. These results indicate some degree of surface heterogeneity and potential multilayer adsorption was possible during the adsorption of Tonalide. This model produces F-value of 296.64 and a Prob > F < 0.0001 further confirms the statistical significance of model. Overall, results suggest that the Langmuir model was adequately describes the adsorption behaviour of Tonalide confirms the monolayer adsorption of Tonalide on homogeneous active sites of nanocomposite.

Reusability and structural stability of the Co-MOF@Ag_2O nanocomposite was treated as very critical parameters to evaluate its practical applicability and cost-effectiveness for large-scale wastewater treatment, particularly in the removal of persistent organic pollutants such as synthetic musk compounds. The successive adsorption–desorption cycles were carried out using Tonalide and Galaxolide

Accepted manuscript

under optimized conditions to assess the reusability potential of nanocomposite. After each adsorption cycle, the nanocomposite was recovered by simple filtration, thoroughly washed with deionized water followed by ethanol (5 mL). Then the adsorbent was dried in a hot air oven at 65 °C for 6 hours to eliminate residual adsorbates and moisture and then the regenerated adsorbent was subsequently used in fresh adsorption runs. These results indicate that the nanocomposite retain its adsorption efficiency effectively over five consecutive cycles with minimal / negligible decrease in removal performance. Beyond the fifth cycle, a gradual decline in adsorption capacity was observed which may be attributed to the possible blockage or saturation of active adsorption sites or the structural degradation of the MOF framework or may be the agglomeration of nanoparticles. These findings highlight that the synthesized nanocomposite exhibit good reusability and operational stability that makes them it a promising and sustainable adsorbent for the repeated removal of musk fragrances from aqueous environment.

Adsorption performance observed in this study was compared with various adsorbents reported for the removal of musk compounds. Results clearly demonstrate the superior efficiency of the synthesized Co-MOF@Ag_2O nanocomposite for the removal of musk compounds in the study. The reported materials mainly rely on oxidative, photochemical, or UV-activated processes that often require high energy input and pose the risk of reactive by-product formation. Whereas the Co-MOF@Ag_2O nanocomposite synthesized in this study offers simpler, safer, and more sustainable adsorption pathway. The well-defined porosity, high surface reactivity, and synergistic metal–oxide interface provide distinct advantage of synthesized Co-MOF@Ag_2O nanocomposites over conventional adsorbents such as activated carbon, modified biochars, and engineered polymeric composites. Moreover, this approach avoids the utilization of hazardous chemicals, specialized reactors, or energy-intensive treatments that make this study more practical and scalable route for removing Galaxolide and Tonalide from contaminated water. Detailed comparison of reported methods and the advantages of present material was summarized in Table S1.

CONCLUSION

In this research, a cobalt-doped magnetic MOF@Ag_2O nanocomposite was successfully prepared through a green synthesis pathway by utilizing the *Ficus carica* L. leaf extract for effective removal of polycyclic musk compounds i.e., Tonalide and Galaxolide from aqueous solutions. The in-depth characterizations establish the crystallinity, nanoscale morphology of nanocomposite with large surface area, and thermal stability and zeta potential stability. Adsorption experiments reveal that under optimized conditions (pH 5 for Tonalide, pH 6 for Galaxolide; 20–30 mg dose; 90 min contact time), the composite achieved over 95 % removal efficiency. Kinetic modeling indicate that the adsorption follows

Accepted manuscript

pseudo-second-order mechanism with high equilibrium adsorption capacities (Q_e: 105.41±0.263 mg/g for Tonalide and 110.10±0.115 mg/g for Galaxolide) and strong chemisorptive interactions that involves π–π stacking, hydrogen bonding, and coordination with active metal sites. The reusability test indicates that the composite can be used effectively for five cycles with little efficiency loss. There should be future studies that will analyse the adsorption efficiency of nanocomposite in the removal of musk compounds in actual wastewater samples and need to investigate the interaction mechanisms involved in the high adsorption efficiency of nanocomposite using sophisticated spectroscopic techniques.

SUPPLEMENTARY MATERIAL

Additional data are available electronically at the pages of journal website: https://www.shd-pub.org.rs/index.php/JSCS/article/view/13717, or from the corresponding author on request.

Acknowledgements: Corresponding author grateful to the Department of Chemistry, Koneru Lakshmaiah Education Foundation, Vaddeswaram for providing the necessary infrastructure and laboratory facilities to carry out this research.

И З В О Д

СИНТЕЗА И ПРИМЕНА МАГНЕТНОГ MOF@Ag_2O НАНОКОМПОЗИТА ДОПИРАНОГ КОБАЛТОМ ЗА АДСОРПЦИОНО УКЛАЊАЊЕ ПОЛИЦИКЛИЧНИХ МОШУСНИХ ЗАГАЂУЈУЋИХ СУПСТАНЦИ

K.T.S.N. TARUN KUMAR[1], PAVANI PEDDI[2], M.V. LAKSHMI[3], CH. RAJYALAKSHMI[4] И VENKATESWARA RAO ANNA[1*]

[1]Department of Chemistry, Koneru Lakshmaiah Education Foundation,Vaddeswaram, Guntur - 522302, A.P., India, [2]Department of Chemistry, FED, PVP Siddhartha Institute of Technology, Kanuru, Vijayawada-520007, A.P, India, [3]Department of Engineering Chemistry, S.R.K.R. Engineering College, Bhimavaram-534204, A.P, India и [4]Department of Basic Sciences, Vishnu Institute of Technology, Bhimavaram- 534202, A.P, India.

Ова студија је усмерена на зелену синтезу, карактеризацију и испитивање адсорпционих својстава MOF@Ag_2O нанокомпозита допираног кобалтом, са циљем ефикасног уклањања полицикличних мошусних мирисних загађујућих супстанци, односно галаксолида и тоналида из контаминиране воде. Методе: Наночестице Ag2O синтетисане су методом зелене хемијске преципитације, уз употребу екстракта листова смокве (**Ficus carica** L.). Co-MOF је добијен солвотермалном координационом методом, док је нанокомпозит Co-MOF@Ag_2O произведен интеграцијом уз примену микроталаса. Нанокомпозит је детаљно окарактерисан применом XRD, FTIR, SEM, TEM, BET, VSM и TGA метода, као и анализом зета-потенцијала. Резултати карактеризације показују успешно формирање нанокомпозита са структуром нанометарских димензија (~26,9 nm) и високом колоидном стабилношћу (−32 mV). XRD анализа потврђује кристалну структуру обе компоненте, Ag_2O и Co-MOF, док EDX анализа показује његов елементарни састав, потврђујући присуство Co и Ag, као и биомолекула пореклом из биљака које доприносе процесу зелене синтезе. Шаржни адсорпциони експерименти су изведени у циљу процене ефикасности уклањања испитиваних супстанци при различитим експерименталним условима. Највећи степен уклањања тоналида постигнут је на pH 5, док је за галаксолид максимално уклањање постигнуто на pH 6, при оптималним дозама адсорбента од 20

Accepted manuscript

mg/100 mL, односно 30 mg/100 mL. Кинетичка испитивања показала су да оба једињења следе кинетички модел псеудо-другог реда, са високим коефицијентима корелације (R^2 = 0,9989 за тоналид и 0,999 за галаксолид), што указује на хемисорпцију као доминантан механизам адсорпције. Вредности адсорпционог капацитета у равнотежи (Q_e) износиле су 105,41 ± 0,263 mg/g за тоналид и 110,10 ± 0,115 mg/g за галаксолид. Нанокомпозит је показао високу могућност поновне употребе, уз очување високе адсорпционе ефикасности током пет циклуса. Резултати рада указују на потенцијалну примену Co-MOF@Ag_2O нанокомпозита као еколошки прихватљивог, високоефикасног и одрживог адсорбента за уклањање стабилних синтетичких мошусних једињења у процесима пречишћавања отпадних вода.

(Примљено 8. јануара; ревидирано 23. фебруара; прихваћено 19. октобра 2026.)

REFERENCES

1. S. Tasselli, M. Rogora, A. Orrù, L. Guzzella, *Environ. Sci. Pollut. Res.* **30** (2023) 109643 (https://doi.org/10.1007/s11356-023-30030-9)
2. R. Harsha, I. Herath, C. Lin, Ch. Subrahmanyam, *Environ. Pollut.* **343** (2024) 123140 (https://doi.org/10.1016/j.envpol.2023.123140)
3. S. F. Ahmed, M. Mofijur, S. Nuzhat, A. T. Chowdhury, N. Rafa, Md. A. Uddin, A. Inayat, T. M. I. Mahlia, H. C. Ong, W. Y. Chia, P. L. Show, *J. Hazard. Mater.* **416** (2021) 125912 (https://doi.org/10.1016/j.jhazmat.2021.125912)
4. W.-L. Li, C. Shunthirasingham, F. Wong, S. A. Smyth, A. Pajda, N. Alexandrou, H. Hung, C.-Y. Huo, T. Bisbicos, M. Alaee, G. Pacepavicius, C. Marvin, *Environ. Sci. Techn.* **58** (2024) 5524 (https://doi.org/10.1021/acs.est.4c00840)
5. C. Chen, L. Shen, B. Wang, X. Lu, S. Raza, J. Xu, B. Li, H. Lin, B. Chen, *Chem. Soc. Rev.* **5** (2025) (https://doi.org/10.1039/D4CS00435C)
6. S. Lal, P. Singh, A. Singhal, S. Kumar, A. P. S. Gahlot, N. Gandhi, P. Kumari, *RSC Adv.* **5** (2024) 3413 (https://doi.org/10.1039/D3RA07982A)
7. V. Manikandan, J. V. Kumar, D. Elango, V. Subash, P. Jayanthi, S. Dixit, S. Singh, *Chem. Rec.* **25** (2025) e202400257 (https://doi.org/10.1002/tcr.202400257)
8. Q. Zhang, H. Yang, T. Zhou, X. Chen, W. Li, H. Pang, *Adv. Sci.* **9** (2022) 2204141 (https://doi.org/10.1002/advs.202204141)
9. S. Tang, Y. Wang, P. He, Y. Wang, G. Wei, *Materials* **17** (2024) 2660 (https://doi.org/10.3390/ma17112660)
10. S. Agatonovic-Kustrin, S. Wong, A. V. Dolzhenko, V. Gegechkori, H. Ku, J. Tucci, D. W. Morton, *J. Chromatogr. A.* **1706** (2023) 464241 (https://doi.org/10.1016/j.chroma.2023.464241)
11. A. S. Gungure, L. T. Jule, N. Nagaprasad, K. Ramaswamy, *Sci. Rep.* **14** (2024) 26967 (https://doi.org/10.1038/s41598-024-75614-8)
12. G. Hootifard, E. Sheikhhosseini, Sd. Ali Ahmadi, M. Yahyazadehfar, *Sci. Rep.* **13** (2023) 17500 (https://doi.org/10.1038/s41598-023-44667-6)
13. X. Dong, M. Zheng, L. Qu, L. Shi, L. Wang, Y. Zhang, X. Liu, Y. Qiu, H. Zhu, *Mar. Pollut. Bul*. **144** (2019) 129 (https://doi.org/10.1016/j.marpolbul.2019.04.046)
14. A. Tadesse, M. Hagos, D. RamaDevi, K. Basavaiah, N. Belachew, *ACS Omega.* ***5*** (2020) 3889 (https://doi.org/10.1021/acsomega.9b03175)

Accepted manuscript

15. J. Santiago-Morales, M. J. Gómez, S. Herrera, A. R. Fernández-Alba, E. García-Calvo, R. Rosal, *Water Research.* **46** (2012) 4435 (https://doi.org/10.1016/j.watres.2012.05.051)
16. Q. Zhang, J. Wang, H. Lyu, Q. Zhao, L. Jiang, L. Liu, *Sci. Total. Environ.* **659** (2019) 1537 (https://doi.org/10.1016/j.scitotenv.2019.01.005)
17. L. Wang L, X. Liu, *Processes* **7** (2019) 95 (https://doi.org/10.3390/pr7020095)
18. L. Hernández-Leal, H. Temmink, G. Zeeman, C. J. N. Buisman, *Water Res.* **45** (2011) 2887 (https://doi.org/10.1016/j.watres.2011.03.009)
19. G. Veneti, T. Chatzimitakos, C. Stalikas, *J. Chromatogr. A.* **1679** (2022) 463375 (https://doi.org/10.1016/j.chroma.2022.463375).
20. H. Praveen, V. Girish Chandran, *J. Thermoplast. Compos. Mater.* **38** (2025) 2670 (https://doi.org/10.1177/08927057251322172)
21. H. Praveen, V. Girish Chandran, *Polym. Bull.* **82** (2025) 4755 (https://doi.org/10.1007/s00289-025-05724-4)
22. H. Praveen, V. Girish Chandran, *J Mater Sci: Mater. Electron.* **34** (2023) 1446 (https://doi.org/10.1007/s10854-023-10884-y)
23. P. Ristić, T. R. Todorović, V. Blagojević, O. R. Klisurić, I. Marjanović, B. Barta Holló, P. Vulić, M. Gulea, M. Donnard, M. Monge, M. Rodríguez-Castillo, J. M. López-de-Luzuriaga, N. R. Filipović, *Cryst. Growth Des.* **20** (2020) 4461–4478 (https://doi.org/10.1021/acs.cgd.0c00287)
24. P. Ristić, N. Filipović, V. A. Blagojević, J. Ćirković, B. Barta Holló, V. R. Đokić, M. Donnard, M. Gulea, I. Marjanović, O. R. Klisurić, T. R. Todorović, *Cryst. Eng. Comm.* **23** (2021) 4799–4815 (https://doi.org/10.1039/d1ce00394a)
25. G. Gonfa, A. Kidanu, S. Akram, B. Lal, G. Kezembayeva, D. O. Bokov, A. Asghari, K. K. Yadav, A. Saravanan, A. Hosseini-Bandegharaei. *Sci Rep.* **15** (2025) 41993 (https://doi.org/10.1038/s41598-025-25998-y).

Accepted manuscript